

# Deep Neural Networks as the Semi-classical Limit of Topological Quantum Neural Networks:

## The problem of generalisation

Antonino Marcianò,<sup>1</sup> Deen Chen,<sup>2</sup> Filippo Fabrocini,<sup>3</sup> Chris Fields,<sup>4</sup> Matteo Lulli,<sup>5</sup> and Emanuele Zappala<sup>6</sup>

<sup>1</sup>*Center for Field Theory and Particle Physics & Department of Physics, Fudan University, Jingwan campus, Jingsan Rd, 200433 Shanghai, China and Laboratori Nazionali di Frascati INFN, Via Enrico Fermi, 54, 00044 Frascati (Rome), Italy, EU\**

<sup>2</sup>*College of Design and Innovation, Tongji University, 281 Fuxin Rd, 200092 Shanghai, China<sup>†</sup>*

<sup>3</sup>*College of Design and Innovation, Tongji University, 281 Fuxin Rd, 200092 Shanghai, China and Institute for Computing Applications "Mario Picone", Italy National Research Council, Via dei Taurini, 19, 00185 Rome, Italy, EU<sup>‡</sup>*

<sup>4</sup>*Allen Discovery Center, Tufts University, 200 College Avenue, 02155 Medford, MA, US<sup>§</sup>*

<sup>5</sup>*Department of Mechanics and Aerospace Engineering, Southern University of Science and Technology, 1088 Xueyuan Avenue, 518055 Shenzhen, China<sup>¶</sup>*

<sup>6</sup>*Yale School of Medicine, Yale University, 300 George Street, New Haven, CT, 06511, USA<sup>\*\*</sup>*

Deep Neural Networks miss a principled model of their operation. A novel framework for supervised learning based on Topological Quantum Field Theory that looks particularly well suited for implementation on quantum processors has been recently explored. We propose the use of this framework for understanding the problem of generalization in Deep Neural Networks. More specifically, in this approach Deep Neural Networks are viewed as the semi-classical limit of Topological Quantum Neural Networks. A framework of this kind explains easily the overfitting behavior of Deep Neural Networks during the training step and the corresponding generalization capabilities.

### I. INTRODUCTION

Deep neural networks (DNNs), i.e. neural networks with several hidden layers, have become popular due to their success in a variety of learning task ranging from molecular design [1] and socioeconomic predictions [2], to machine translation [3] and approximating partial differential operators [4]. However, our fundamental understanding of this technology has lagged far behind. DNNs are largely considered to be "black box" systems to the extent that, on one side, they miss a principled model of their operation while, on the other side, the internal operation of DNNs cannot be easily read out by human beings. The first issue is mainly related to our limited understanding of how DNNs achieve those generalization capabilities that let us state that they are able to learn (whatever "learning" means here) while the second has to do with the difficulty of interpreting

the operational behavior of a non-linear weighted model trained over hundreds of thousands of inputs that contribute microscopically to the final configuration of the network. These issues together constitute the main technical challenge for achieving a fair, accountable, and transparent Artificial Intelligence (AI), with the first generally considered under the rubric of verifiability (see [5, 6] for recent reviews) and the second generally considered under the rubric of XAI (see [5–7] for recent reviews).

The objective of this paper is to deal with the first issue by developing and validating a principled model of generalization in DNNs. Our approach thus differs from post-hoc or example-based approaches (see e.g. discussion in [7]) by seeking a tractable mathematical model of the function  $f$  computed by some DNN system following training with a training set  $S$ . In this sense, our study falls in the field of generalization theory. The generalization ability of DNNs is not yet understood despite the rich literature concerning the topic and it is still a mystery [8–20]. A principled approach to a trustable AI clearly requires understanding how DNNs generalize, and hence how they fail to generalize correctly in particular situations. A principled model of generalization will enable performance validation at the theoretical level, as opposed to merely the empirical one. In particular, a principled model of DNN generalization will hopefully enable the designer of Machine Learning (ML) applications to meet specific, pre-established generalization and performance objectives. As Kevin Hartnett [21] has written in Quanta Magazine:

---

\*Electronic address: [marciano@fudan.edu.cn](mailto:marciano@fudan.edu.cn)

†Electronic address: [deenchen@tongji.edu.cn](mailto:deenchen@tongji.edu.cn)

‡Electronic address: [fabrocini@tongji.edu.cn](mailto:fabrocini@tongji.edu.cn)

§Electronic address: [fieldsres@gmail.com](mailto:fieldsres@gmail.com)

¶Electronic address: [lulli@sustech.edu.cn](mailto:lulli@sustech.edu.cn)

\*\*Electronic address: [emanuele.zappala@yale.edu](mailto:emanuele.zappala@yale.edu), [zae@usf.edu](mailto:zae@usf.edu);

We acknowledge Krid Jinklub for useful comments. AM acknowledges support by the National Science Foundation of China, through the grant No. 11875113, the Shanghai Municipality, through the grant No. KBH1512299, and by Fudan University, through the grant No. JJH1512105. ML acknowledges the support from National Science Foundation of China grant No. 12050410244. (Corresponding author: Filippo Fabrocini.)

When we design a skyscraper, we expect it will perform to specification: that the tower will support so much weight and be able to withstand an earthquake of a certain strength. But with one of the most important technologies of the modern world, we are effectively building blind. We play with different designs, tinker with different setups, but until we take it out for a test run, we do not really know what it can do or where it will fail.

We do not really know, in fact, after one or even several test runs: it always remains the case that the “next” generalization problem will reveal failure. A principled approach for studying generalisation in DNNs is to prove a generalisation bound which is typically an upper bound on the test error based on some features of the training set. Unfortunately, finding tight bounds has proven to be a difficult challenge so far.

To further motivate our goal of a principled approach to generalisation, it is useful to contrast it with state-of-the-art example-based, post-hoc explanations [7]. As emphasized in [22], post-hoc methods are, effectively, applications of experimental cognitive psychology techniques to ML systems. Such techniques have an obvious weakness: a successful ML system may be detecting patterns in both training and test data that human observers cannot detect, as AlphaFold [23] appears to do. ML systems work with uninterpreted inputs; what we regard as “image” data, for example, are just bit patterns to a ML system. In particular, they have no access to the object categorizations – the semantics – imposed by humans. Experiments such as in [24] show that humans are very poor at processing images as layouts of pixels, independently of object identification and categorization. It is not clear whether explanation in the usual sense is possible when ML systems detect patterns that humans cannot detect, and hence have no semantics for, particularly patterns that conflict with typical human object categories. Our approach is independent of categories or other imposed semantics; we model the process of generalisation in the abstract, not its outcomes in particular cases. Hence our approach – like any verification approach – can underlie and give confidence to, but does not replace, example-based explanation techniques that are aimed at humans, and thus must employ shared human semantics. A two-part solution of this kind, if successful, can be expected to have a beneficial social impact since it will improve the trustworthiness of AI systems in the interest of an Artificial Intelligence (AI) “for social good”, as a number of high-profile initiatives in the Ethical AI field have emphasized (e.g. Asilomar AI Principles, Montreal Declaration for Responsible AI, EU Ethics Guidelines for Trustworthy Artificial Intelligence, IEEE Global Initiative for Ethical Considerations in Artificial Intelligence and Autonomous Systems, etc.; see [25–27]

for discussion).

We address the generalisation problem by leveraging results coming from Topological Quantum Field Theory (TQFT). TQFT is used to construct a topological version of Quantum Neural Networks (QNNs) named Topological Quantum Neural Networks (TQNNs) [28]. TQNNs differ from conventional QNNs [29, 30] by allowing the number of “layers” and their connection topology to vary arbitrarily, provided only that the input and output boundary conditions are preserved. The full generality of the TQNN framework as a representation of computational processes acting on classical data to yield classical outputs has been recently proven [31]. We use this framework to explain the generalisation issues in DNNs by adopting a quantum physics approach according to which the generalisation capabilities of DNNs are the analogue of the semi-classical manifestation of quantum effects or, more specifically, of the topological encoding achieved by TQNN. This allows us, in particular, to “read off” detected topological invariants independently of their semantics, and hence independently of their detectability by human observers.

The plan of the paper is the following. In Sec. II we remind the reader about the state of the art of neural networks and provide motivations for our study. In Sec. III we summarize the novel strategy rooted in the framework provided by TQFT, namely TQNN. In Sec. IV we discuss generalisation within the TQNN framework. In Sec. V we provide a dictionary correlating DNN and TQNN notions. In Sec. VI we outline possible perspectives associated with the new strategy developed. Finally, in Sec. VII we offer some preliminary conclusions based on the TQNN models.

## II. MOTIVATIONS AND THEORETICAL BACKGROUND

We will recall here a few essential notions of ML with the aim of introducing the problem of generalisation in DNNs. A learning algorithm receives as input a training set  $S$ , sampled from an unknown distribution  $D$  and labelled by a function  $f'$ , the restriction to  $S$  of some unknown target function  $f$  defined on  $D$ . Hence we represent the learning algorithm as an operation:

$$\mathcal{L} : (r, f') \mapsto f, \quad (1)$$

where  $r$  is the (presumably random) function implemented by the network prior to training. The target function  $f$  is unknown because we do not, in fact, know how humans classify data sets, e.g. how humans identify dogs in images. The goal of the algorithm  $\mathcal{L}$  (implementing e.g. some form of error backpropagation) is to construct, using  $S$  as data, a classifier or predictor  $h_S$  belonging to a class of hypotheses  $H$  that minimizes the error  $L_D$  (the true error) with respect to the unknown

$D$  and  $f$ . The error of a classifier  $L_D(h)$  is the probability that it does not predict the correct label for an unseen instance  $x$ , i.e. not present in the training set  $S$ , drawn from  $D$ . As  $f$  is not known, what counts as a “correct” label is ill-defined; in practice, it is defined ostensibly by a human choice. Since both  $D$  and  $f$  are unknown, we will calculate the training error rather than the true error based on the dataset  $S$ . The problem will thus correspond to the minimization of the empirical risk function  $R_{\text{emp}}(h)$ , namely the estimate of the *Empirical Risk Minimization* (ERM). The empirical risk function,

$$R_{\text{emp}}(h) = \frac{1}{n} \sum_{i=1}^n L(h(x_i), y_i), \quad (2)$$

is defined as the average over a training set of the loss function  $L$ , which is such that  $L \neq 0$  if  $h(x_i) \neq y_i$  and  $L = 1$  otherwise. For a given class  $H$  and a training sample  $S$ , the  $ERM_H$  learner uses the ERM rule to choose a predictor  $h \in H$ , with the lowest possible error over  $S$ . Formally,  $ERM_H(S) \in \text{argmin}_{h \in H} L_S(h)$ . The empirical error of  $h$  is then its average error over the training set  $S$ , while the generalisation error is its expected error based on the distribution  $D$ . The accuracy of this expectation clearly depends on the representativeness of  $S$  as a sample of  $D$ , and hence the representativeness of the training labels  $f'$  as a sample of the unknown target function  $f$ .

If  $S$  does not adequately represent  $D$ , the ERM rule might easily lead to overfitting, with the consequence that the model will generalize poorly. Therefore, we need to search for conditions that allow the learning algorithm to show good performance on the training set  $S$  without underperforming on the underlying data distribution  $D$ . In other words, we will need to find the right balance between underfitting and overfitting. Typically the balance will be achieved by selecting the most appropriate capacity [65] of the class  $H$  and/or resorting to regularization techniques (e.g. early stopping, weight decay, dropout, etc.). For instance, a traditional approach, rather than fixing in advance the complexity of the class, consists in building a hierarchy of classes  $H_c$  splitting the complexity of a richer class  $H$  in which  $c$  is the complexity parameter. A method that follows this approach is given by Support Vector Machines (SVMs) where the complexity of the class is chosen based on the data by making use of Reproducing Kernel Hilbert spaces (RKHS) [32]. A methodology of this kind is looking for the best trade-off between the minimization of the empirical risk and the complexity of the class  $H_c$ .

The goal of generalisation theory is to explain and justify why and how minimizing the computable empirical error (the training error) is a reasonable approach to minimize the non-computable error (the test error) by analyzing the generalisation gap *test error* – *training error*. This challenge stems from the dependence of the

predictor  $h_S$  on the same dataset  $S$  in the case of both the training error and the test error. However, as noted above, the training set  $S$  might not be sufficient to direct the learner towards a good classifier if the training sample is insufficiently representative of the underlying distribution  $D$  that the learner intends to capture. In a ML model one is by definition more interested in the generalisation error rather than in the empirical error to the extent that our main goal is evaluating the performance of the model on the unseen cases, i.e. on  $D \setminus S$ . If we look at the problem from this point of view, then the challenge comes from the mismatch between the optimization task consisting of minimizing the empirical or training risk and the machine learning task consisting of minimizing the true or test risk insofar as:

$$L_{D,f}(h) = P_{x \sim D}[h(x) \neq f(x)] = D[\{x : h(x) \neq f(x)\}],$$

where the error of such  $h$  is the probability of randomly drawing an example  $x$ , according to the distribution  $D$ , for which  $h(x) \neq f(x)$  and the error is measured with respect to the probability distribution  $D$  and the correct labeling function  $f$ . Here  $P$  is the probability of a random variable, and  $x \sim D$  represents sampling  $x$  according to  $D$ . This probability can also be expressed in measure theory terminology. Formally, given a member,  $A$ , of some  $\sigma$ -algebra of subsets of the domain  $\mathcal{X}$ , the probability distribution  $D$ , assigns a number,  $D(A)$ , which determines how likely it is to observe a point  $x \in A$ .

The dependence of the predictor  $h$  on the training data set  $S$  has led to the definition of several examples of complexity measures providing bounds on the test error or on the sample-complexity. An instance of these measures are the VC-dimension or the Rademacher complexity. In particular, if the VC-dimension provides an upper bound on the test error, the Rademacher complexity measures the richness of a class of predictors with respect to a probability distribution. These results provide bounds on the test error that depend on the complexity or capacity of the class of functions  $H$ . In this sense, generalisation theory and capacity control are strictly related. Capacity control consists in using models that are rich enough to get good fits without using those which are so rich that they overfit.

Yet, the empirical success of DNNs, which are typically overparametrised models [33], challenges the traditional complexity measures insofar as, according for instance to the VC-dimension, the discrepancy between training error and generalisation error is bounded from above by a quantity that grows at least linearly as the number of adjustable parameters grows but shrinks as the number of training examples increases, with the consequence that the traditional complexity measures tend to control the capacity by minimizing the number of parameters [34–36]. Moreover, experimental results prove that DNNs that have been trained to interpolate

the training data achieve a near-optimal test result even when the training data have been corrupted by a massive amount of noise [37]. As Poggio et al. [38] write, the main puzzle of DNN revolves around the absence of overfitting despite large overparametrization and despite the large capacity demonstrated by zero training error on randomly labeled data. It is, in other words, the fact that DNNs can implement an operation  $\mathcal{L}' : (r, g) \mapsto f$  that (at least approximately) correctly generalizes to the desired  $f$  from a function  $g$  that is not the restriction of  $f$  to the training set  $S$ , but rather a noise function, namely a function of randomized data, on  $S$ .

Historically the puzzle has been raised by a seminal paper from Zhang et al. [39]; see also [40]. This paper has shown that successful deep model classes have sufficient capacity to memorize randomised data sets while having the ability to produce zero training error for particular natural datasets (e.g. CIFAR-10). The authors also empirically observed that explicit regularization on the norm of weights seemed to be unnecessary to obtain small test errors, in contradiction to “traditional wisdom”. In the case of DNNs, the large capacity of the model looks sufficient to memorize the training data by brute force. However, this behavior conflicts with the traditional idea of generalisation since learning by explicit memorisation of training examples should not imply generalisation capabilities. Generalising is traditionally understood as learning some underlying rule associated with the data generation process, i.e. learning some compact representation of the training function  $f'$ , and therefore being able to extrapolate that rule from the training data to new unseen data. Moreover, as we have already mentioned, a result of this kind is a challenge to traditional complexity measures and, in general, to computational learning theory since none of the existing bounds produces non-trivial results for interpolating solutions of the sort generated by such DNN models.

Several efforts have recently focused on achieving non-vacuous generalisation bounds for DNN models [14, 41, 42]. In the light of this situation, Belkin et al. [43] propose to subsume the traditional U-shaped risk curve describing the trade-off between underfitting and overfitting with a double-descent risk curve. In their view, when the number of parameters  $N$  is much smaller than the sample size  $n$ , i.e.  $N \ll n$ , the traditional complexity measures assume that the training risk is close to the test risk. However, according to the double descent risk curve that the authors propose, by increasing progressively  $N$  and thus by increasing the class capacity, the model will also increase the function classes until they are rich enough to achieve zero training error, with the consequence of constructing progressively near-perfect fit functions that typically show a smaller norm and, consequently, are simpler in the sense of the Occam’s razor. A view of this kind contradicts the

traditional framework according to which, by increasing the class capacity, the predictors will perfectly interpolate the data with the consequence of achieving an overfitting regime and, therefore, of having a very high generalisation risk. Yet, as the authors state, increasing further the function class capacity beyond this point, leads to decreasing test risk, typically below the risk achieved when balancing underfitting and overfitting under the traditional approach (see Figure 1).

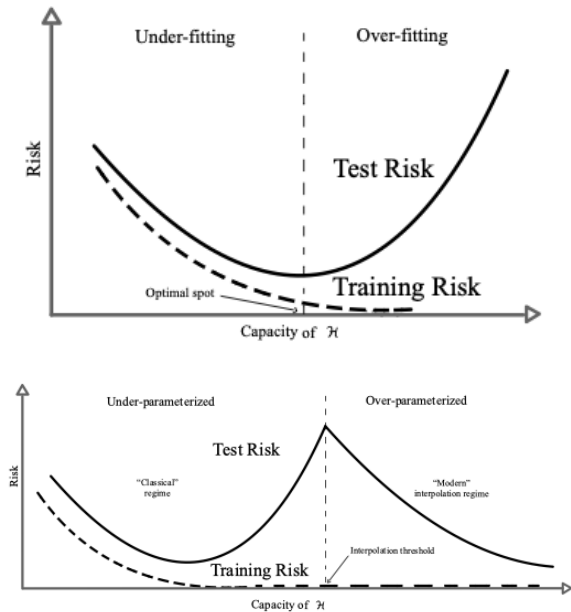


FIG. 1: Risk curves in classical and modern regime.

This view matches recent results from Poggio et al. [38] and Bartlett et al. [32] according to which overparametrization leads to “benign overfitting” in which an accurate level of generalisation is achieved despite a near-fit to training data. In particular, according to the authors, overparametrization enables gradient techniques to impose regularization implicitly while leading to accurate predictions despite their overfitting behaviour. A behavior of this kind will prefer matrices showing a smaller norm, a result that, according to a number of a scholars, matches the thesis that the generalisation performance depends on the size of the weights rather than on the number of weights [15, 44–47]. A thesis of this kind will guide our approach as well, even though it will be embedded into a theoretical framework totally different from complexity theory. In particular, we wish to unveil the source of generalisation in DNNs by deploying techniques borrowed from Topological Quantum Physics (TQP). Our proposal is based on two hypotheses, both grounded on results coming from TQP and, in particular, from Topological Quantum Field Theory (TQFT): a) TQNNs generalise by encoding topological, not just metric, invariants that characterize their training sets; b) DNNs can be represented as the semi-classical limit of a class of TQNNs. As we will see, in the TQNN frame-



work, generalisation is achieved as the selection of topological invariants that are captured in the TQP approach by the linking and knotting quantum numbers assigned to graphs and to the 2-complexes of TQNNs.

### III. TQNN IN TQFT

Before tackling the issue of generalisation, elaborating on the results attained by Zhang et al., [39, 48], we summarize in this section the novel strategy rooted in the framework provided by TQFT [28]. This is an effective quantum theoretic approach that offers the pathway to address the problem of generalisation. We will show that the origin of this problem can be related to the topological encoding within the network structure, achieved through path selection and parameter optimisation, which coincide, in the classical limit, with the training of classical neural networks. In addition, we argue that training TQNNs naturally implements, through the selection of topological features, an optimisation over the architecture of the corresponding classical neural networks in the semi-classical limit. This is in stark contrast with the classical case, where the architecture of the network is fixed beforehand, and the weights are learned during training. Consequently, optimal architecture selection and generalisation become, in the semi-classical limit, different interpretations of the same underlying TQNN procedure.

Within the framework of TQNN introduced in [28], both the elements of the training and test samples are associated to quantum states — the boundary states of the underlying TQFT — that are colored with irreducible representations of Lie groups. In practice, these boundary states are represented by spin-networks that are dual to triangulations of a manifold. They encode the discretisation of space-time in that they combinatorially represent the continuous underlying manifold. In this context, the  $G$ -bundle structure of the manifold is encoded in terms of group elements on the edges of the spin-network. Quantum states are represented by cylindrical functionals of the boundary group elements that are associated to the input data, and are supported on boundary graphs (1-complexes). Output boundary states represent instead the TQNN ability to react to solicitations provided by the input (training/test samples). The functorial evolution from input to output boundary states is captured by 2-complexes, which realise the sum over histories proper of path integral in quantum mechanics. The physical scalar product between boundary states is then used to produce a numerical output that later determines the train and test errors.

On the one hand, the “input to output” functorial evolution realises a sum over all the geometries of the system, similarly to the Misner-Hawking integral (see [49]). Cer-

tain geometries resonate giving rise to dominating terms in the output of the TQNN. In other words, the structure of the data induces TQNNs to select certain geometries. On the other hand, the learning procedure here consists of an optimisation on the parameters of the heat kernel corresponding to coherent spin-network states (see e.g. [50]). Therefore, the resonances are determined by the integral over the histories learned during training. This duplicity reflects the double role of learning in TQNNs, where both the architecture and the weights are learned, as previously mentioned.

Therefore our working framework, developed within an extended effective framework that follows the very same axioms of quantum field theories [28], hinges on the following steps:

1. To data we associate (possibly a superposition of) spin-networks through some encoding procedure (see [28]). The spin-networks are determined by the irreducible representations that label their edges and live in the boundary Hilbert space of the TQFT theory.
2. The generic boundary states are characterized by two classes of parameters, which we dub as *topological* and *metric* parameters. The former ones are determined by the topology of the graph supporting the spin-networks and the topology of the manifolds, whose simplicial decompositions are dual to the spin-networks. These are quantum invariants obtained through state sums of admissible states. The metric parameters relate to the differential structure of the manifold and appear in the spin-network formalism from the fact that spin-network edges support the connection of the underlying manifold. These parameters are captured by the spin of the representation itself.
3. Information provided by the training samples, together with the analogical definition of training and test error, in terms of the internal product of boundary quantum states, allows to fix the functorial structure of the bulk of the TQNN, namely the topological structure of the TQNN 2-complex. This procedure determines the topological parameters, since it gives the quantum groups in terms of which the topological invariants are expressed. We also observe that the weights of the boundary coherent states are learned during the training process.
4. The topological parameters are enough to capture the pattern underlying the training set; whenever the “information” about the topology specified by the training data is not sufficient and/or noise exceeds the possibility to individuate topological structures, an interpolating pattern which does not select specific topological features is then deployed.

5. The metric parameters are individuated by the Gaussian weights associated to the coherent group elements assigned to the TQNN states. In the semi-classical limit these weights correspond to the matrix weights of DNNs. For instance, in [28] we recover the perceptron as the semi-classical limit of a specific TQNN.
6. The measure of the Hilbert spaces associated to the links, that are deemed to be equivalent to the training sample set, characterises the minimal amount of information flow required to achieve pattern identification: if not enough information is provided by the group elements, which is determined through the association of spin-network states to input data, not enough information is provided to reconstruct the topological invariants.
7. The “richness” or “energy” of the irreducible representation sets allows to “switch on” the links, and thus the nodes and the topological linking and knotting invariants, only for non-trivial (non-zero) values of the spin representations. Thus, the analogue of the minimal length in theories of quantum gravity, or Planck length, is the minimal spin, or information bit, in the framework of [28].

Relying on this framework, we propose in the next section that generalisation, within the context of classical DNNs, emerges from the optimisation in the semi-classical limit of the TQFT path-integral (states’ sum) deployed to estimate the classifier. Moreover, topological features, including topological invariants (states’ sum) of the underlying TQFT and graph connectivity of spin-network boundary states, are essential elements to achieve generalisation. In fact, as argued in more detail in Section IV, we have that learning corresponds to singling out preferred topologies in the form of resonances in the transition amplitudes. These are dominant terms in the partition function induced by the path-integral of the TQFT.

Change of the graphs’ topology is achieved at the (infinite number of quantum) hidden layers by vertices structures implementing the TQNN evolution. Through the topological features of the 1- and 2- complexes, the TQNN can capture the topological invariants from the training sets. On the other hand, parameter optimisation in the states’ sum corresponds to the individuation of the semi-classical limit of the quantum theory: the “classical” path is individuated by the extremisation of the action of the theory in the sum over histories; fluctuations around that path still enable to achieve generalisation, as a minimisation of the training error.

Within this novel picture, topological and metric data captured by the TQNNs’ structure increase the class capacity and thus ultimately the function classes of the quantum ML models under scrutiny. Indeed, refining the triangulation/tessellation of geometric manifolds underlying the description of data ensembles results into

an increase — either in the simplicial skeletons extracted by manifolds triangulation/tessellation or in their dual 1-complexes — of the topological connectivity of the graphs on which TQNNs are supported. While increasing the ensemble of metric data saturates the risk curve of Figure 1 to provide a standard U-shaped form, the complexity of the TQNNs graph structure that encodes the topological data provide an asymptotic improvement of generalisation. For TQNNs graph structures that are not sufficiently enough rich, the model, only characterised by the flow of metric data along the links of the 1-complexes, undergoes overfitting as the ensemble of metric informations increases. Nonetheless, increasing the graph complexity through enlarging the topological data ensembles enables metric data to increase function capacity. This suggests that the one-dimensional curves that appear in Figure 1 should be replaced by a curve that takes into account two different independent classes for the parameters characterising the models under scrutiny, to be represented respectively on the axes for the metric and the topological complexity, as depicted in Figure 2.

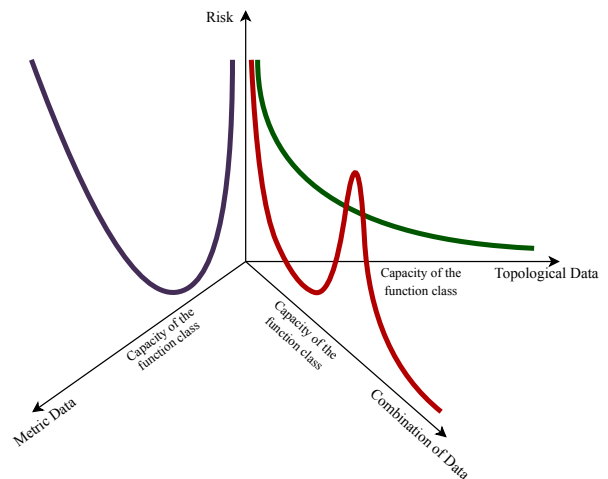


FIG. 2: Topological and metric complexity.

#### IV. GENERALISATION IN THE FRAMEWORK OF TQNN

Our perspective relies on the conjecture that generalisation happens as the analogue of the macroscopic manifestation of quantum mechanical effects. Specifically, generalisation can be addressed as the manifestation of topological (quantum) encoding achieved in TQNN and classical path-selection.

The texture of the webs of vertices and edges, which is determined by the data and captures the topology of the (triangulated) manifold as its dual simplicial complex, concretely implements a higher level topological pattern [28], unveiling which path coincides with the procedure of learning. Generalisation is consequently achieved in this framework as the selection of topological invariants,

the most adequate to the achievement of a specific task. These topological invariants are captured in the TQP framework by the linking and knotting quantum numbers assigned to graphs and to the 2-complexes of TQNN.

### A. The notion of generalisation in DNNs as semi-classical limit of TQNNs

Let us now consider in detail the issue of generalisation in TQNNs, and consequently attempt to answer the problem raised in [48] for DNN. When a coherent states representation of the Hilbert space is chosen, this corresponds to the selection of a family of states, in the training sample dataset, which is characterized by a random assignment of the irreducible group representation labels. The representation labels are in turn peaked around the labels of the coherent states that capture the mean values of the observable quantities and are determined through the quantum annealing procedure. This represents therefore a natural definition of labels' randomisation in the training set. Label randomisation can be compared to randomly defining the elements of the Hilbert space, as this corrupts the correspondence between underlying data and correct label.

A classical DNN has only to learn the function  $f'$  in Eq. (1), which specifies example input-output pairs; it has no access to the "intrinsic" structure of the training examples. TQNNs, however, are sensitive to such intrinsic structure in the form of topological features. The structure of TQNNs naturally encode topological charges through the functorial quantum dynamics ensured by the 2-complexes, which create either vertices and then functions of  $j$ -representation and intertwiner quantum numbers, i.e. amplitudes, or other topological charges encoded in the knotting and linking of the edges in the bulk of the 2-complex.

For clarity, let us consider the case of the TQNN analogue of the classical architecture of *perceptron*. As shown in [28] Section 5, the classical perceptron is recovered as the semi-classical limit of a TQNN. In fact, considering the composability properties of TQNN, inherited from the functoriality of TQFTs (the Atiyah axioms), it follows that this procedure describes also the *multilayer perceptron* (MLP) in the semi-classical limit. In particular, we argue that the semiclassical limit, which singles out the classical trajectories from the infinite amount of quantum trajectories, corresponds to the minimisation of the weight vector. For perceptrons, the components of the weight vector are determined by the minimisation of the loss functional or the learning task at hand. In the framework of TQNN, the weight vector is substituted by the set encoding the values of the action at the nodes and links of the boundary states — see [28] Section 5 — and at the infinitely many quantum hidden layers interpolating among the boundary states. The minimisation

process that constitutes learning, therefore, in this case consists in the minimisation of a Feynman path-integral (associated to the TQFT), and it therefore amounts to selecting the dominant contributors to the infinitely many paths.

When the action is minimised, the weight amplitudes of the path integral are maximised. On the other hand, minimisation of the action ensures selection of the classical paths. In turn, tiny fluctuations around these minima correspond to the semi-classical paths nearest to the classical ones.

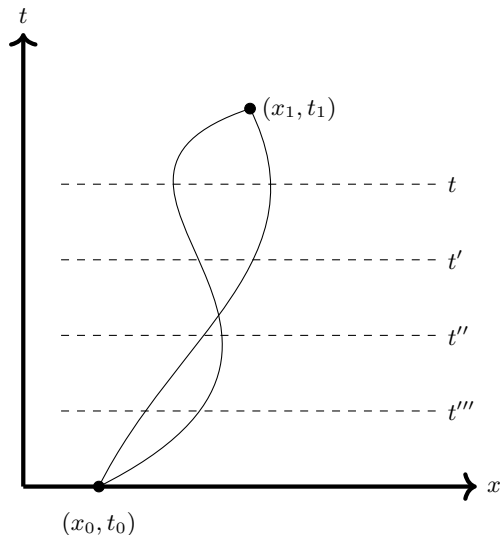


FIG. 3: Possible paths in  $xt$ -plane.

The case of DNNs like MLPs consists of composing (via functoriality of the given TQFT) single units as in the case of the perceptron. The paradigm described above is substantially unchanged.

### B. Generalisation for the special case of one-node states

The simplest example we can provide is the one that concerns the quantum mechanics of a one-particle system. This would correspond within the DNN/TQNN correspondence to an architecture where the boundary states consist of a single node. Hidden (DNN) and quantum (TQNN) layers differ in this picture by their cardinality, i.e. the number of copies interpolating among the boundary (one-node) states, and their size, i.e. the number of nodes at each intermediate layer. This difference is substantially prompted by the fact that classical DNNs have a fixed architecture, which corresponds to a single path in the Feynman formulation, while TQNNs superpose all the possible paths. Hidden layers in DNNs are indeed finite in number of copies and finite in size, while quantum layers can be also infinite in number of copies and in size. DNNs would then account for a finite sum over a finite set of intermediate steps,

while quantum mechanics realizes a sum over infinite possible quantum states. Furthermore, DNNs assign probability weights among the edges connecting one-node states to nodes of the hidden layers, while TQNNs assign to the internal edges probability amplitudes, i.e. complex numbers the absolute value square of which are probabilities. The infinite number of quantum layers between input and output layers arises from the fact that any TQFT used to define a TQNN is invariant under triangulation changes, i.e. it is invariant under Pachner moves, and therefore arbitrary refinements of the simplicial decomposition between input and output are all taken into account by the TQFT. A related perspective concerns the Matveev-Piergallini moves, as described in [51] for the quantum group  $\mathcal{U}_q(\mathfrak{sl}_2)$ .

Representing then boundary states with one-particle quantum states of quantum mechanics, we can associate

$$\begin{aligned} |\text{in}\rangle &\rightarrow |x_{\text{in}}, t_{\text{in}}\rangle, \\ |\text{out}\rangle &\rightarrow |x_{\text{out}}, t_{\text{out}}\rangle, \end{aligned} \quad (3)$$

where the Cartesian coordinate  $x$  labels the particle position (in a one-dimensional linear space) and  $t$  denotes the time parameter deployed to follow its dynamical evolution.

Suppose now to partition  $t \in [t_{\text{in}}, t_{\text{out}}]$  in  $N - 1$  steps of interval  $\Delta t = (t_{\text{out}} - t_{\text{in}})/(N - 1)$ . While in TQNNs we take the limit  $N \rightarrow \infty$ , when considering the semi-classical limit for DNNs  $N$  is fixed to be a finite number. Now, from the perspective of TQNNs, we estimate the classifier  $\mathcal{Z}_\ell(x_{\text{in}}, x_{\text{out}})$  as the partition function of the one-particle system, with  $x_{\text{in}}$  and  $x_{\text{out}}$  labelling the boundary states, and  $\ell$  labelling the infinite set of all the possible paths connecting  $x_{\text{in}}$  to  $x_{\text{out}}$ , as determined by the partition function of the underlying TQFT. This means that

$$\mathcal{Z}_\ell(x_{\text{in}}, x_{\text{out}}) = \langle x_{\text{out}}, t_{\text{out}} | x_{\text{in}}, t_{\text{in}} \rangle = \langle x_N, t_N | x_1, t_1 \rangle. \quad (4)$$

Now we can decompose  $\mathcal{Z}_\ell(x_{\text{in}}, x_{\text{out}})$  into the product of the corresponding intermediate steps (using the functoriality of the theory) and get

$$\begin{aligned} \langle x_N, t_N | x_1, t_1 \rangle &= \int dx_{N-1} \int dx_{N-2} \cdots \int dx_2 \times \\ &\langle x_N, t_N | x_{N-1}, t_{N-1} \rangle \times \\ &\langle x_{N-1}, t_{N-1} | x_{N-2}, t_{N-2} \rangle \cdots \langle x_2, t_2 | x_1, t_1 \rangle. \end{aligned} \quad (5)$$

Within each interval of time  $\Delta t$ , we consider the Feynman amplitude

$$\langle x_k, t_k | x_{k-1}, t_{k-1} \rangle = \frac{1}{w(\Delta t)} e^{iS(k, k-1)}, \quad (6)$$

where

$$S(k, k-1) \equiv \int_{t_{k-1}}^{t_k} dt L_{\text{classical}}(x, \dot{x}), \quad (7)$$

is the classical action evaluated in the  $k$ -th time interval  $\Delta t$ , with  $k = 1, \dots, N - 1$ .

Notice that the generic  $k$ -th amplitude has the meaning of a propagator from the point  $\{x_k, t_k\}$  to the point  $\{x_{k-1}, t_{k-1}\}$ , since the generic intermediate states  $|x_k, t_k\rangle$  and  $|x_{k-1}, t_{k-1}\rangle$  evolve according to the Schrödinger picture, i.e.

$$\begin{aligned} \langle x_k, t_k | x_{k-1}, t_{k-1} \rangle &= \langle x_k | e^{-\frac{i}{\hbar} H \Delta t} | x_{k-1} \rangle \\ &= K(x_k, t_k; x_{k-1}, t_{k-1}). \end{aligned} \quad (8)$$

By construction, the propagator  $K(x_k, t_k; x_{k-1}, t_{k-1})$  satisfies the Schrödinger time-dependent wave equation, and the property

$$\lim_{t_k \rightarrow t_{k-1}} K(x_k, t_k; x_{k-1}, t_{k-1}) = \delta(x_k - x_{k-1}). \quad (9)$$

The propagator hence determined is nothing but the Green's function of the time-dependent Schrödinger wave equation, i.e.

$$\begin{aligned} \left[ H(x_k) - i\hbar \frac{\partial}{\partial t_k} \right] K(x_k, t_k; x_{k-1}, t_{k-1}) &= \\ \delta(x_k - x_{k-1}) \delta(t_k - t_{k-1}), \end{aligned} \quad (10)$$

where  $H(x_k)$  is the differential representation of the Hamiltonian operator in  $x_k$ , and with boundary condition

$$K(x_k, t_k; x_{k-1}, t_{k-1}) = 0, \quad \forall t \notin [t_{k-1}, t_k]. \quad (11)$$

In (6), the factor in front of the exponential can only depend on the time interval  $\Delta t$ . Being independent from the potential to which the particle is subjected, it can be estimated by calculating from (10) the propagator of a non-relativistic free particle, with Hamiltonian  $H = \frac{1}{2}m\dot{x}^2 = -\frac{\hbar^2}{2m}\nabla^2$ , hence finding the expression

$$\frac{1}{w(\Delta t)} = \sqrt{\frac{m}{2\pi i \hbar \Delta t}}. \quad (12)$$

We can now consider the limit for which the partition acquires an infinite amount of “filters”, and hence the time interval  $\Delta t$  shrinks to zero. Within this limit, each  $k$ -th amplitude will contribute according to

$$\langle x_k, t_k | x_{k-1}, t_{k-1} \rangle = \sqrt{\frac{m}{2\pi i \hbar \Delta t}} e^{\frac{i}{\hbar} S(k, k-1)}, \quad (13)$$

providing as a final expression for the transition from  $|\text{in}\rangle$  to  $|\text{out}\rangle$  the relation

$$\begin{aligned} \langle x_N, t_N | x_1, t_1 \rangle &= \lim_{N \rightarrow \infty} \left( \frac{m}{2\pi i \hbar \Delta t} \right)^{\frac{N-1}{2}} \int dx_{N-1} \int dx_{N-2} \\ &\cdots \int dx_2 \prod_{k=2}^N e^{\frac{i}{\hbar} S(k, k-1)}. \end{aligned} \quad (14)$$



By the definition of  $S(k, k-1)$  in (7), and denoting the sum over the paths as  $\mathcal{D}[x(t)]$ , namely

$$\int_{x_1}^{x_N} \mathcal{D}[x(t)] = \lim_{N \rightarrow \infty} \left( \frac{m}{2\pi i \hbar \Delta t} \right)^{\frac{N-1}{2}} \int dx_{N-1} \times \int dx_{N-2} \cdots \int dx_2 \quad (15)$$

we find the celebrated expression for the Feynman path-integral

$$\langle x_N, t_N | x_1, t_1 \rangle = \int_{x_1}^{x_N} \mathcal{D}[x(t)] e^{\frac{i}{\hbar} \int_{t_1}^{t_N} L_{\text{classical}}(x, \dot{x})}. \quad (16)$$

When a free particle is considered, one can observe that the semi-classical limit corresponds to the minimization of the action, hence to imposing the stationarity of the norm of  $\vec{X} = p/\sqrt{2m}$ . Taking into account relativistic invariance, in a  $d+1$ -dimensional space-time manifold, the vector  $\vec{X} = \vec{p}/\sqrt{2m}$  will turn out to be  $d$ -dimensional. Thus the dimensionality of the vector  $\vec{X}$  equals the space dimension of the ambient space-time manifold.

The interpretation we provide here is straightforwardly preserved every time we consider a Lagrangian that is quadratic in the configuration variables and their momenta. More in general, we can resort to a symplectic geometry analysis to identify in full generality the norm of the vector  $\vec{X}$  in terms of an Hermitian inner product. This latter is generated by the symplectic structure associated to the manifold — see e.g. Refs. [52–54] — and corresponds to the norm of the action of the space-time translation generator applied to the configuration fields of the system. In fact, when the Lagrangian presents higher order terms, one can proceed by perturbing the path integral as shown for example in [55] for Chern-Simons theory. This allows to compute higher order terms in the perturbation as described above. Moreover, this paves the way to further parametrizations that can be learned during training in the form of topological charges. This situation, albeit very interesting, will not be considered explicitly in the present article.

Notice furthermore that once manifolds with Lorentzian signature are taken into account, the extremization of the action would not correspond to a minimization of  $\vec{X}$ , being the system hyperbolic. In this latter case, the extremization of the action on a hyperbolic manifold provides the classical trajectories/geodesics of the systems, namely the classical paths that instantiate generalisation within the DNNs framework.

Therefore the estremisation of the weights, whose role in generalisation has been commented in Sec. II referring to [15, 44–47], is replaced in this picture by the minimisation of the action. This latter in turns

corresponds to maximise the probability amplitudes in the path integral formulation of a classifier.

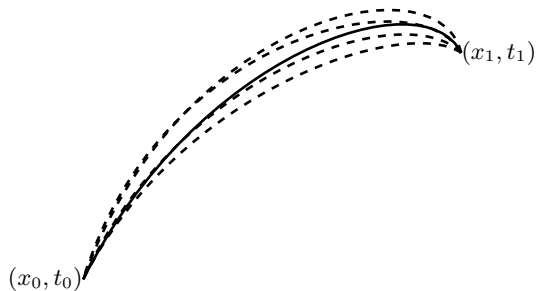


FIG. 4: Predominant paths in the  $\hbar \rightarrow 0$  limit.

We are now in the position to express our thesis on the generalisation process. The partition function that determines the TQFT used by the TQNN utilises a superposition of all colorings of the input/output pairs, and intermediate states amplitudes, as shown above, give the single probabilities (upon taking moduli squared) of the single transitions of color configurations that constitute the summands of the partition function. Optimization here shows the dominant terms in the superposition function, according to the given underlying ground truth. Thus generalisation emerges as an artifact of the semiclassical limit: DNNs structures are only able to represent fixed 2-skeletons within the 2-complex evolution of TQNNs. These are nevertheless the most dominant contributions to the path integral for the TQNNs, which is in general realised by the topological quantum neural 2-complexes (TQN2Cs), summing over all the quantum histories. This simple case with boundary states with single nodes is generalised directly to the case of spin-networks with higher number of nodes, where the reasoning still holds true. In fact, this formulation was used in [28].

### C. Generalisation for TQNNs

We have so far addressed the process of generalisation for DNNs as the semiclassical limit of TQNNs, with particular emphasis on the case of single-node boundary states. However, a more general question naturally arises, regarding the notion of generalisation for TQNNs. In other words, we ask (and provide an answer to) the question of what a TQNN learns, and therefore what the generalisation procedure looks like in the quantum case.

Although the notion of TQNN seems to share similarities with graph neural networks (GNNs), we observe that the two methods are substantially different. In fact, GNNs are determined by a fixed geometry and, in addition, such geometry determines the way information

is processed through the learning procedure (message passing). On the contrary, TQNNs have no fixed geometric structure, but they are applied through their defining functorial rules on graphs that correspond to spin-networks, and therefore elements of the boundary Hilbert space, via some pre-determined assignment (see [28] Section 4 for such a concrete correspondence). Information from the boundary states is then processed according to the defining rules of the given choice of TQFT — quantum  $\mathfrak{sl}_2$  in the case discussed in detail in [28]. Since a TQFT is supported on the bulk manifold and it is independent on the triangulation used, it follows that the information contained in the boundary is processed according to methods that are not determined by the geometric structure of the supporting boundary graph, as it happens in the case of message passing for GNNs. This is a fundamental perspective that TQNNs leverage to generalise.

TQNNs evolve according to the dynamics dictated by topological quantum field theories (TQFTs). Transition amplitudes calculated according to TQFTs instantiate classifier rules that interconnect TQNN states. As in [28], we focus on  $BF$ -extended theories, which is a theoretical framework general enough to encode Yang-Mills gauge theories as well as effective field theories. Specifically, TQNNs are states of the kinematical Hilbert space of TQFTs. Their topological features are easily captured once their expansion on the spin-networks basis is taken into account. Nonetheless, an equivalent expansion in the multi-loop basis is also possible [56], which renders less evident the connectivity of graphs and thus (some of) their topological features. Such expansion is obtained by unraveling the Jones-Wenzl symmetrizer (projector) placed on each edge of the input boundary, following the definition of spin-network state. For our purposes, it suffices to consider the expansion of TQNNs on the spin-networks basis, found e.g. in [57].

We consider a manifold  $\mathcal{M}$ , and a submanifold  $\mathcal{S}$  such that  $\mathcal{M} = \mathcal{M}_0 \cup_{\mathcal{S}} \mathcal{M}_1$ , for submanifolds  $\mathcal{M}_i$ ,  $i = 0, 1$ , with  $\partial\mathcal{M}_i = \mathcal{S}$ . The one-complexes (graphs)  $\gamma$  are then considered as embedded in  $\mathcal{S}$ . A generic TQNN state can be expanded on the elements of the spin-network basis, each one being supported on a generic graph  $\gamma \in \mathcal{S}$ . In turn, each spin-network state is defined as a triple  $\Psi = (\gamma_{\Psi}, \rho, \iota)$  consisting of a graph  $\gamma_{\Psi} \in \mathcal{S}$ , an irreducible representation  $\rho_l$  of  $G$  for each link  $\gamma_i \in \gamma_{\Psi}$ , an intertwiner  $\iota_n$  for each node  $n$  such that

$$\iota_n : \rho_{l_1} \otimes \cdots \otimes \rho_{l_n} \rightarrow \rho_{l'_1} \otimes \cdots \otimes \rho_{l'_n}, \quad (17)$$

where the links incoming into the node  $n$  have been denoted as  $l_1, \dots, l_n$ , and the links outgoing from the node  $n$  have been denoted with  $l'_1, \dots, l'_n$ .

Without loss of generality, we may directly focus on a generic spin-network state  $\Psi$ . Suppose now that  $\Psi$  is the spin-network state associated to some boundary initial

state derived from a data-point, namely

$$|\text{in}\rangle \rightarrow |\Psi\rangle, \quad (18)$$

where the correspondence is determined according to some given rule as in Section 4 of [28], for example. Similarly, introduce the boundary final state  $\Phi$ , i.e.

$$|\text{out}\rangle \rightarrow |\Phi\rangle. \quad (19)$$

Generic TQNN states  $\Psi$  and  $\Phi$  encode two types of data: topological data, namely the connectivity of the graphs  $\gamma_{\Psi}$  and  $\gamma_{\Phi}$ ; metric data, corresponding to the assignments of quantum numbers to the links and nodes of the graph  $\gamma_{\Psi}$  and  $\gamma_{\Phi}$ , namely the irreducible representations  $\rho_l$  for each link  $l \in \gamma_{\Psi}$  or  $l \in \gamma_{\Phi}$ , and the intertwiner quantum number  $\iota_n$  for each node  $n \in \gamma_{\Psi}$  or  $n \in \gamma_{\Phi}$ . Both the topological and metric data that are encoded in  $\Psi$  and  $\Phi$  are processed by the classifier  $\mathcal{Z}$ . This latter is nothing but the matrix element of the quantum evolution operator — in the path integral representation — that associates the initial state  $|\text{in}\rangle = |\Psi\rangle$  to the final state  $|\text{out}\rangle = |\Phi\rangle$ . The action of the evolution operator/classifier on the boundary states amounts to the assignment of the transition amplitude  $\langle \Phi | \Psi \rangle_{\text{phys}}$ . Here, the subscript “phys” is reminding us that the amplitude is calculated in terms of the dynamics of the specific TQFT taken into account, thus it differs from the scalar product  $\langle \Phi | \Psi \rangle$  calculated in the kinematical Hilbert spaces to which the TQNN states  $\Psi$  and  $\Phi$  belong. In practice, the transition amplitude is one of the summands appearing in the partition function that defines the chosen TQFT.

Once a specific TQFT is selected, and a gauge group  $G$  is fixed, the states of the TQNN can be represented as cylindrical functionals

$$\Psi(H_l) := \langle H_l | \Psi \rangle \quad (20)$$

that depend on the holonomies  $H_l \in G$  along the links  $l \in \gamma_{\Psi}$ . Holonomies are group elements of  $G$  that realize the parallel transport along a path  $\gamma \subset \mathcal{S} \subset \mathcal{M}$ , with respect to the connection  $A$  over the principle  $G$ -bundle. The graph  $\gamma_{\Psi}$  here represents a discretization of the underlying manifold, and its links represent small paths in the manifold — cf. the notion of edge in lattice gauge theory. Denoting path-ordering with  $P$ , the parallel transport of a vector in a representation  $\rho$  of  $G$  reads

$$H_l = P e^{\int_l A_a \tau^a}, \quad (21)$$

with  $a$  an index in the adjoint representation of  $G$  and  $\tau^a$  a representation of the generators of  $G$ .

The classifier quantum amplitudes can be derived for an extended  $BF$ -theory over a  $G$ -bundle. We consider a local trivialization on  $\mathcal{M}_d$ , and denote the curvature of the  $G$ -connection  $A$ , which is a  $\mathfrak{g}$ -valued 1-form, with a

$\mathfrak{g}$ -valued 2-form  $F$ ,  $\mathfrak{g}$  standing for the Lie algebra of  $G$ . A frame field  $B$  can be introduced, as the field conjugated to  $A$ , and such that the symplectic structure is fulfilled

$$\omega((\delta A, \delta B), (\delta A', \delta B')) = \int_S \langle \delta A \wedge \delta B' - \delta A' \wedge \delta B \rangle, \quad (22)$$

where the conjugated fields have been restricted on an initial (in time, for the Lorentzian case) slice  $\{0\} \times S$  of  $\mathcal{M}_4$ , and we have denoted the trace over the internal indices with  $\langle \dots \rangle$ . Notice that the frame field  $B$  is a  $\mathfrak{g}$ -valued 2-form. This allows to write consistently the action of the  $BF$ -extended theory over either a Riemannian or a Lorentzian 4-dimensional manifold  $\mathcal{M}_4$  as

$$\mathcal{S}_{\text{BF}}^{\text{ext.}}[A, B] = \int_{\mathcal{M}_4} \langle B \wedge F + \lambda_1 B \wedge B + \lambda_2 B \wedge \star B \rangle, \quad (23)$$

with  $\lambda_1, \lambda_2 \in \mathbb{R}$  bare coupling-constants. For  $\lambda_1 \neq 0$  and  $\lambda_2 = 0$ , the theory is still topological, and corresponds to the Crane-Yetter model, whose quantization involves recoupling theory of quantum groups — see e.g. the notable example that corresponds to  $G = SU(2)$ . For  $\lambda_1 = 0$  and  $\lambda_2 \neq 0$ , the theory is non-topological and corresponds on-shell to a Yang-Mills action with internal gauge group  $G$ . Furthermore, when the Lorentzian case with  $G = SL(2, \mathbb{C})$  is taken into account, and  $\lambda_1$  is promoted to a multiplet of scalar fields, with a pair of symmetric indices that are in the adjoint representation of  $SL(2, \mathbb{C})$ , one can recover the Einstein-Hilbert-Holst action of gravity for 4-dimensional space-time [31].

For the sake of simplicity, we focus on the topological realization of the  $BF$ -theory that corresponds to selecting  $\lambda_1 = \lambda_2 = 0$ . The equations of motions then read

$$F = 0, \quad d_A B = 0, \quad (24)$$

where  $d_A$  denotes the covariant derivative with respect to the  $G$ -connection  $A$ .

The classifier evolution is easily recovered in terms of the instantiation of the curvature constraint  $F = 0$  in a physical projector  $\mathcal{P}$ . In turn, the implementation of the physical projector  $\mathcal{P}$  was discussed in [58], where it was shown how to make sense of the formal expression

$$\mathcal{P} = \int \mathcal{D}N \exp(\imath \int_S \langle N \widehat{F} \rangle), \quad (25)$$

with  $N$  a  $\mathfrak{g}$ -valued Lagrangian multiplier and  $\imath = \sqrt{-1}$  imaginary unit.

In particular, the curvature constraint  $F = 0$  can be implemented in the physical amplitudes among spin-network states according to

$$\langle \Psi, \Phi \rangle_{\text{phys}} = \langle \mathcal{P}\Psi, \Phi \rangle. \quad (26)$$

A local patch  $\Sigma \in S$  can be considered that is provided with cellular decomposition composed of squares of

infinitesimal coordinates length  $\delta$ . The regularized curvature constraint then reads

$$F[N] = \int_{\Sigma} \langle NF(A) \rangle = \lim_{\delta \rightarrow 0} \sum_{p^j} \delta^2 \langle N_{p^j} F_{p^j} \rangle, \quad (27)$$

in which  $p^j$  labels the  $j$ -th plaquette and  $N_{p^j}$  is the discretization of the  $\mathfrak{g}$ -valued Lagrangian multiplier  $N$ , evaluated at an interior point of the plaquette  $p^j$ .

The holonomy  $H_{p^j}[A]$  around the plaquette  $p^j$  is a  $G$  group-element that casts

$$H_{p^j}[A] = \mathbb{1} + \delta^2 F_{p^j}(A) + \mathcal{O}(\delta^2), \quad (28)$$

which implies

$$F[N] = \int_{\Sigma} \langle NF(A) \rangle = \lim_{\delta \rightarrow 0} \sum_{p^j} \delta^2 \langle N_{p^j} H_{p^j}[A] \rangle. \quad (29)$$

The regularized expression for the action of the physical projection operator immediately follows. This enters the physical scalar product of spin-network states:

$$\begin{aligned} \langle \Psi, \Phi \rangle_{\text{phys}} &= \lim_{\delta \rightarrow 0} \left\langle \prod_{p^j} \int \mathcal{D}N_{p^j} \exp(\imath \langle N_{p^j} \widehat{H}_{p^j} \rangle) \Psi, \Phi \right\rangle \\ &= \lim_{\delta \rightarrow 0} \left\langle \prod_{p^j} \delta(H_{p^j}) \Psi, \Phi \right\rangle. \end{aligned} \quad (30)$$

Having reminded the structures of TQNNs and their TQFT evolution in terms of TQNN2C classifier, we can now address the problem of generalisation in this extended theoretical framework. We may assume that the size of the training data is sufficient to select or, better, to learn specific paths in the boundary graphs and bulk 2-complexes within the most general available TQNN architecture. These paths are characterised by different types of associated non-perturbative topological charges, which in turn provide the sub-structures involved in the generalisation process, as a subset supported on general 2-complexes. More concretely, these correspond to summands in the partition function of the TQFT that is used to define the TQNN, and determine the dominating contributions to the topological invariants. In other words, certain intrinsic algebro-geometric features emerge that characterize the learning of the TQNN.

The BF-extended formulation provided by (23) encode Yang-Mills theories over a  $G$ -bundle for the choice  $\lambda_1 = 0$  and  $\lambda_2 = 2g_{\text{YM}}^2$ . Thus the optimization of the classifier will correspond to the minimization of the classical Yang-Mills action, namely

$$\mathcal{S}_{\text{YM}} = \frac{1}{2g_{\text{YM}}^2} \int_{\mathcal{M}_4} \langle F \wedge \star F \rangle. \quad (31)$$

Cast in terms of the spacetime components, with  $a$  denoting the indices of the adjoint-representation of

the algebra  $\mathfrak{g}$ , the Lagrangian density  $F^a_{\mu\nu}F^{a\mu\nu}$  turns out to be proportional to the norm of a tensor on a hyperbolic manifold with Lorentzian signature.

Path selection is attained by minimisation of the classical action and extremisation of the path-integral formulation of the classifier, which is naturally realised in the semi-classical limit, in a way that is reminiscent of the free energy principle formalism [59–62].

The topological charges that are switched on over the learning process and correspond to the configurations that extremise the action, together with the corresponding metric properties, implement effectively the generalisation process. In this sense, our approach is expected to provide a solution to the problem as raised by Zhang et al, 2016. In particular:

- The randomisation of the labels of a TQNN state will not induce overfitting as a consequence of the encoding of information achieved by the TQNN through the topological features and topological invariants. The quantum nature of the TQNN will induce fluctuations around values of the parameters to be estimated. Nonetheless, these fluctuations are small in the semi-classical limit.
- However, a DNN architecture will be trapped into an overfitting regime until memorising the training examples by brute force, since by definition of DNNs the training error vanishes — the variance for the  $j$  scale as  $1/\sqrt{j}$ . In other words, associating a DNN to a set of spin-networks evaluated into coherent group elements, the corresponding training error is zero.

Thus, brute-force learning is not possible for a TQNN, since the topological information of the input/output states would automatically make the transition amplitude vanish, most of the time, with random labelling.

## V. A DICTIONARY FOR TQNNs

Along the lines specified in [28], we propose once again in this section a dictionary between TQNNs and the most relevant notions in standard machine learning, including DNN theory.

It is useful to restrict our focus to supervised learning. This latter task implements learning of a usually unknown function  $f : D \rightarrow Y$  that maps an input set  $D$  to an output set  $Y$ , and is based on a training set  $S \subset D$  and a function  $f' : S \rightarrow Y$  that specifies example input-output pairs. Considering  $f : X \rightarrow Y$  as the (presumably random) function  $r$  implemented by the network before the training, the learning algorithm can be specified, as in Eq. (1), as an operation  $\mathcal{L} : (r, f') \mapsto f$ . A statistical learning framework for supervised learning can be then introduced, along the lines of [63], as well as some standard definitions for DNN that we list below.

- **Sample complexity:**  
It represents the number of training-samples (i.e.  $Card(S)$ ) that a learning algorithm needs in order to learn successfully a family of target functions.
- **Model capacity:**  
It is the ability of the model to fit a wide variety of functions; in particular, it specifies the class of functions  $\mathfrak{H}$  (the hypothesis class) from which the learning algorithm  $\mathcal{L}$  can choose the specific function  $h$ .
- **Overfitting:**  
A model is overfitting when the gap between training error and test error is too large; this phenomenon occurs when the model learns the training function  $f'$  but  $\mathcal{L}$  incorrectly maps  $(r, f') \mapsto h \neq f$ , i.e. the trained network generalises to the wrong function  $h$  and fails to predict future observations (i.e. additional samples from  $D$ ) reliably. The training function  $f'$  has been merely “memorised” to the extent that  $h$  is incorrect (e.g. random) on  $D$  outside of the training sample  $S$ .
- **Underfitting:**  
A model is underfitting when it is not able to achieve a sufficiently low error on the training function  $f'$ ; this phenomenon occurs when the model does not adequately capture the underlying structure of the training data set and, therefore, may also fail to predict future observations reliably.
- **Bias:**  
It is the restriction of the learning system towards choosing a classifier or predictor  $h$  from a specific class of functions  $\mathfrak{H}$  (the hypothesis class).
- **Empirical Risk Minimisation (ERM):**  
It consists in minimising the error on the set of training data (the “empirical” risk), with the hope that the training data is enough representative of the real distribution (the “true” risk).
- **Generalisation:**  
It is conceived as the ability of the learner to find a predictor, i.e. an embedding  $S \rightarrow D$ , which is able to enlarge successfully its own predictions from the training samples to the test or unseen samples.

These notions can be reformulated into the dictionary of TQNNs.

- **Sample complexity:**  
It is a measure of the Hilbert-space of the entire spin-network state that is supported on a specific graph  $\Gamma$ . It is then dependent on the connectivity of the graph (nodes and links of each graph, i.e. the multiplicity of connectivity that characterizes the graph  $\Gamma$ ) and on the dimensionality of the Hilbert spaces connected to each link and node. In



this sense complexity, once extended to the different classes of graphs corresponding to the training set, provides a measure of the entropy of the set. Therefore, in the TQNN framework, the notion of “complexity” has a wider meaning than its counterpart in DNN, for which the sample complexity is nothing but the size of the training set. This is summarised in the expression for the dimension of the Hilbert space  $\mathcal{H}_\Gamma$  of the (whole) spin-network supported on  $\Gamma$ , namely

$$\dim[\mathcal{H}_\Gamma] = \oplus_{j_l} \otimes_n \otimes_{l \in \partial n} \dim[\mathcal{H}_{j_l}].$$

This directly encodes both the size of the maximal graph where the input/output states live, as well as the algebro/analytical structure used in the TQFT from which the corresponding TQNN arises, as encoded by the dimensionality of the Hilbert spaces  $\mathcal{H}_j$ , for instance;

- **Model capacity:**

It is now distinguished in topological model capacity and metric model capacity, the latter being the extension of the definition provided for DNNs to the context of TQNNs.

i) **Topological model capacity:** It is quantified in terms of the interconnectivity of the graph  $\Gamma$ . It depends on the topological structure of the graphic support  $\Gamma$  of the spin-network states, and neither on the dimensionality of the Hilbert space of the irreducible representations nor on the intertwiner quantum numbers, respectively assigned to each link and node of  $\Gamma$ ; in other words, it depends on the total valence  $V$  of  $\Gamma$ , defined in terms of the valences  $v_n$  of each node of  $\Gamma$  through the expression

$$V = \sum_n v_n;$$

ii) **Metric model capacity:** At fixed graph  $\Gamma$ , it depends on the dimensionality of the Hilbert space of the irreducible representations and intertwiner quantum numbers assigned to  $\Gamma$ ;

iii) **Combined model capacity:** It combines the topological and metric capacity, so as to mimic the standard DNN notion of model capacity. It provides a representation of the double Belkin curve as in 2, which fits Figure 1.

- **Overfitting:**

As pointed out in Section III, in the semi-classical limit, the integrals that allow us to compute the transition amplitudes that characterise a TQFT are interpreted as a “sum over all the geometries” of the ground topological manifold, where the integrand is some approximation of the Einstein-Hilbert action. During the learning process, then a TQNN learns how to select certain geometries with respect to certain others in order to maximise certain transition amplitudes corresponding to “a more suitable”

classification. The information available to make this selection during the learning process is that given by the metric data, namely the irreducible representations and intertwiner quantum numbers assigned to the TQNNs graphs, and by the connectivity of the input graphs/spin-networks and their given correlation  $f'$  with the label set  $Y$ . Keeping metric data fixed, if  $f'$  is insufficiently representative of the target function  $f$ , the TQNN may only partially capture the topological structure of the full input set  $D$  and therefore be unlikely to classify correctly spin-network states that are not part of, or are significantly dissimilar from those contained in, the training set  $S$ . Conversely, when connectivity is kept fixed, overfitting follows the standard behaviour of DNNs. Then a U-shaped risk curve as in Figure 1 describes the trade-off between underfitting and overfitting;

- **Underfitting:**

It represents the converse of the overfitting scenario. The geometries that have been selected in the learning process do not correspond to the graphs  $\Gamma$  at the starting point. Less information channels (links) are present, and lower dimensionality of the information channels (dimensions of the Hilbert space associated to each holonomy) as well. As a consequence, the TQNN cannot fit the training set and may therefore also fail to predict future observations reliably;

- **Bias:**

It amounts to the predisposition of the spin-network to account for a specific set of data; it depends on the topological structure of the spin-network states, encoded in the connectivity properties of input  $\Gamma$ 's and on the specific realisation of the TQNN quantum state, i.e. on the weight of the quantum state on the spin-networks basis elements of the Hilbert space.

- **Empirical Risk Minimisation (ERM):**

It is the variance of the Gaussian distribution of the irreducible representations assigned to the holonomies on the links in the semi-classical limit, i.e.

$$\text{ERM} := \sum_l \frac{(j_l - \bar{j}_l)^2}{2L},$$

with  $L$  equal to the total number of links.

- **Generalisation:**

It is the behavior of the system in response to test or unseen data analogous to a functor (amplitude) either from a boundary spin-network to another boundary spin-network, or from a boundary spin-network to a complex number. This is determined by the geometries that have been selected as the most representative of a certain training sample

during the learning process. This is in practice captured by the parameters that give higher relevance, in the integral computing the transition amplitudes in a TQNN, to certain boundary transitions, while suppress others. These parameters are determined by (i) connectivity of 1- and 2-complexes (nodes and links, vertices and edges respectively), (ii) linking and knotting (e.g. for loops in a different Hilbert space representation), and (iii) states' sum (as a global topological charge, invariant under refinement of the triangulation, i.e. invariant under refinement of the data/group elements/intertwiners assigned to the links and the nodes). In [28], parameters enter the expression for the amplitudes thanks to the coherent states formalism. For  $U_l$  elements of a group  $G$  we may resort to the formula for the partition function of the model:

$$\mathcal{Z}_{\mathcal{C}}(U_l) = \int_{\text{SU}(2)^{2(E-L)-V}} dU_{v(e)} \int_{\text{SU}(2)^{V-L}} dU_f \times \prod_f \mathcal{K}_{f^*}(U_{e^*}, U_f), \quad (32)$$

where the ‘‘face amplitude’’ casts

$$\mathcal{K}_{f^*}(U_{e^*}, U_f) \equiv \sum_{j_{f^*}} \Delta_{j_{f^*}} \chi^{j_{f^*}} \left( \prod_{e^* \in \partial f} U_{e^*} \right) \times \prod_{e^* \in \partial f} \chi^{j_{f^*}}(U_f). \quad (33)$$

Finally, from the definitions of the present article, we can provide the meaning of Learner’s input and output in the context of TQNN.

- Learner’s input:

i) The domain set  $D$ : It corresponds to links  $l$  and nodes  $n$ , and attached holonomies  $U_l$  and invariant tensors  $\iota_n$  respectively along the links and at the nodes: it is concisely denoted as a state of the Hilbert space of the theory:

$$\Psi_{\Gamma; \{j_l\}, \{\iota_n\}}[A] \equiv \Psi_{\Gamma}(U_l, \iota_n) := |\Gamma; \{j_l\}, \{\iota_n\}\rangle;$$

ii) The label set  $Y$ : It is a set of topological charges and quantum numbers, with which the 2-complex is endowed; for instance, recalling the group-isomorphism  $\pi_3(S_3)$ , for the mapping individuated by the homotopy group  $\pi_3(S_3) = \mathbb{Z}$  the winding number  $w$  is defined as the integral over the  $\text{SU}(2)$  group element

$$w = \frac{1}{24\pi^2} \int_{\text{SU}(2)} dU;$$

iii) The training data  $S$ : it is the union of the (initial) boundary colored graphs together with the topological invariants associated to them through the TQN2C functorial action.

- Learner’s output:

It is a prediction rule, i.e. the TQN2C that identifies the topological charges of the boundary states (training/test samples) and thus implements the classifier; for  $\gamma$  a 1-complex supporting a disjoint boundary state, and  $\mathcal{C}$  a 2-complex with boundaries  $\partial\mathcal{C} = \gamma$ , the classifier is captured by the probability amplitude that results from the internal product

$$\mathcal{A} = \langle \gamma; \{j_l\}, \{\iota_n\} | \mathcal{Z}_{\mathcal{C}, \partial\mathcal{C}=\gamma}; \{j_l\}, \{\iota_n\} \rangle,$$

or, once the physical projector  $\mathcal{P}$  has been determined,  $\mathcal{A} = \langle \psi_{\text{out}} | \mathcal{P} \psi_{\text{in}} \rangle$ , for generic boundary states  $\psi_{\text{in}}$  and  $\psi_{\text{out}}$ .

These definitions illustrate, in a very explicit way, the difference between how a TQNN ‘‘sees’’ the input and label sets – and hence the semantics that it assigns to these sets – and how we, as human engineers, see them. From an XAI perspective, the semantics assigned by the TQNN is effectively uninterpretable. Hence as noted above, what our current approach provides is not an explanation of how generalisation has worked in any particular case, but rather an assurance, up to relevant conditions, that it has worked.

## VI. PERSPECTIVE

The main contributions in dealing with the problem outlined by Refs. [39, 48] can be subdivided into two classes : (i) theoretical approaches that try to understand the generalisation issue by proving a generalisation bound on the test error; (ii) phenomenological approaches motivated by experimentation (as concerns a review of these approaches, see e.g. [64]).

Further elaborating on the consequences of the results attained by [48] a novel strategy has been developed in [28] and here that is rooted on the analogue framework provided by TQFT. This is an effective quantum theoretic approach that offers the pathway to address the problem of generalisation. The origin of this latter has been here related to the topological encoding of the input degrees of freedom by the network structure, achieved through pattern selection and parameter optimisation, in the semiclassical limit. The perspective we have then pushed forward here relies on the conjecture that generalisation happens as the analogue of the macroscopic manifestation of quantum effects.

A canonical experiment shedding light on our proposed outlook was carried out by Philipp Lenard, who unveiled the existence of the photoelectric effect. The occurrence of this effect, which only happens at frequencies of the impinging electromagnetic radiation (photons) that are above a certain threshold, provides a macroscopic manifestation of the existence of a quantised energy gap between electronic bounded and valence states,

occurring in electric conductive materials.

This was indeed the framework adopted by Albert Einstein, who achieved a theoretical understanding of such a semiclassical effect grounding it on features of the newly developed theory of quanta. Analogously, generalisation can be addressed as the manifestation of a topological (quantum) encoding achieved by TQNNs. The texture of the webs of vertices and edges, which capture the topological structures of the graphs dual to the input data, implements the pattern [28]. For instance, the skeleton graph dual to the letter 'L' differs topologically from the one dual to the number '8', but metric properties alone distinguish among the number '8' and the symbol ' $\infty$ '.

Generalisation is achieved in the TQNNs framework as a selection, induced by the quantum algorithm, of topological features that are the most adequate to the achievement of a specific task. These topological features are captured by the connectivity of graphs in the boundary states and of the vertices of the 2-complexes. Thus in our proposed picture, the analog of the quantum states of the photoelectric effect – the electrons that appear either in bounded or in valence energy levels, and the photons impinging the condenser's plates of the conductor metal in the Lenard experiment – are the quantum states represented by the cylindrical functionals of the boundary group elements (labelling the input data). These functionals are supported on the boundary graphs (1-complexes), and it is their functorial evolution that is captured by the TQN2C classifiers. Output boundary states represent instead the TQNN's ability to react to perturbations imposed by — effectively, the queries posed by — the input training sets and test samples. The measure of success, for both training and test measures, is provided by the internal product among the boundary states, which is instantiated through the TQN2C functor, accounting for the evolution of the TQNN states [28].

The novelty of our theoretical approach, in particular with respect to recent inspiring studies on the TQNN framework [28, 31], allows to consider a richer architecture that enables to associate machine learning concepts entailing complexity to the topological features that are coded therein. These properties include not only the inter-connectivity of the edges belonging to the graphs, but possibly also associated linking and knotting numbers, and the topological invariant properties of the 2-complexes spanned by the graphs' evolution [28, 31].

Within this framework, generalisation emerges from the optimisation of the topological structures, topological invariants (states' sum) and quantum numbers (topological parameters), while the other parameters, which we may call metric, eventually instantiate effective macroscopic thresholds, such as in the photoelectric effect. Indeed, switching metric parameters on, does

trigger the emergence of the topological features too — see [28] for the details of the dual graphs selection out of the input data. Change of the graphs' topology is then achieved at the hidden layers by vertices structures implementing the TQNN evolution through the TQN2C. Furthermore, the volume of the input data set, increasing with the number of links and nodes, to which holonomies and intertwiner tensors respectively are associated, will play the analogue of the intensity of the radiation in the photoelectric effect (number of photons). While the dimensions of the spin-representations, assigned to the boundary TQNN states, namely the dimension of the Hilbert spaces associated to each link and node, will play an analogous role to the frequencies of the electromagnetic radiation.

Through the definition of this architecture, TQNNs can capture the topological invariants from the training sets, which enables the identification of the correct output, once test samples are deployed. This happens through minimisation and optimisation of the classical action, namely by stationarising the path integral representation of the TQN2C classifiers. This procedure is reminiscent of the free energy principle [59–62]: in the semiclassical limit the most important contributions to the path-integral evaluation of the classifier are the paths that are closest to the classical ones.

Asymptotically, in the semiclassical limit, a finite sample of labels suffices to the success of the generalisation process [28]. This observation suggests a different novel comprehension of the problem of generalisation. Indeed, we have also to remind that, along Zhang et others' work, the generalisation process is independent on the regularisation of the dimensionality of the label sets that are involved. The proposed resolution of the problem may be then naturally achieved through the architectures of the TQNN states, as pointed out in [28], while accounting for a class of TQNN states that are solely supported on graphs and 2-complexes of reduced connectivity.

## VII. CONCLUSIONS

Moving from the innovative framework of [28], we tackled the most relevant theoretical issue related to DNNs: how is it possible that DNNs are able to generalise and, therefore, learn? Understanding how generalisation works may allow to build a principled model of the operation of Deep Learning architectures. On the other hand, delving into the DNNs generalisation process from the perspective of topological quantum physics can provide the key to unprecedented technological implementations.

Considering first the heuristic case of one-node states, which can be treated in full analogy with standard quantum mechanics, and then extending the analysis to

multi-node states of a quantum version of graph neural networks, i.e. topological quantum neural networks, we have shown that the origin of the problem of generalisation can be related to the topological encoding within the quantum graph neural network structure, achieved through path selection and parameter optimisation that corresponds to the semi-classical limit on quantum theories.

Our proposed explanation may have a social and economic impact as well to the extent that it improves the trustworthiness of AI systems, and their practical and industrial applications. We further emphasize that the innovative flavour of our analysis comes from its own interdisciplinary features, which achieve constructing a bridge between traditional ML, with particular regard to DNNs, topological quantum physics and quantum field theory, and materials science.

- 
- [1] M. H. Segler, M. Preuss, and M. P. Waller, *Nature* **555**, 604 (2018).
- [2] J. L. Abitbol and M. Karsai, *Nature Machine Intelligence* **2**, 684 (2020).
- [3] A. Vaswani, N. Shazeer, N. Parmar, J. Uszkoreit, L. Jones, A. N. Gomez, Ł. Kaiser, and I. Polosukhin, in *Proc. NIPS* (2017), vol. 30.
- [4] Z. Li, N. Kovachki, K. Azizzadenesheli, B. Liu, K. Bhattacharya, A. Stuart, and A. Anandkumar, in *Proc. ICLR* (2021).
- [5] J. M. Wing, *Communications of the ACM* **64**, 64 (2021).
- [6] S. Seshia, D. Sadigh, and S. S. Sastry, *Communications of the ACM* **65**, 56 (2022).
- [7] W. Samek, G. Montavon, S. Lapuschkin, C. J. Anders, and K.-R. Müller, *Proceedings of the IEEE* **109**, 247 (2021).
- [8] N. S. Keskar, D. Mudigere, J. Nocedal, M. Smelyanskiy, and P. T. P. Tang, in *Proc. ICLR* (2017), 1609.04836.
- [9] D. Arpit, S. Jastrzebski, N. Ballas, D. Krueger, E. Bengio, M. S. Kanwal, T. Maharaj, A. Fischer, A. C. Courville, Y. Bengio, et al., in *Proc. ICML* (PMLR, 2017), pp. 233–242, arXiv:1706.05394.
- [10] L. Dinh, R. Pascanu, S. Bengio, and Y. Bengio, in *Proc. ICML* (PMLR, 2017), pp. 1019–1028.
- [11] G. K. Dziugaite and D. M. Roy, in *Proc. UAI* (2017).
- [12] E. Hoffer, I. Hubara, and D. Soudry, in *Proc. NIPS* (2017), pp. 1729–1739.
- [13] D. Krueger, N. Ballas, S. Jastrzebski, D. Arpit, M. S. Kanwal, T. Maharaj, E. Bengio, A. Fischer, and A. Courville, in *Proc. ICLR Workshop* (2017), pp. 1–4.
- [14] B. Neyshabur, S. Bhojanapalli, D. McAllester, and N. Srebro, in *Proc. NIPS* (2017), pp. 5947–5956, 1706.08947.
- [15] B. Neyshabur, S. Bhojanapalli, and N. Srebro, in *Proc. ICLR* (2018).
- [16] L. Wu, Z. Zhu, and W. E, in *Proc. ICML Workshop* (2017).
- [17] R. Shwartz-Ziv and N. Tishby, arXiv 1703.00810 (2017), URL <https://arxiv.org/abs/1703.00810>.
- [18] H. W. Lin, M. Tegmark, and D. Rolnick, *Journal of Statistical Physics* **168**, 1223 (2017).
- [19] A. Wang, H. Zhou, W. Xu, and X. Chen, arXiv, 1708.05029 (2017), URL <https://arxiv.org/abs/1708.05029>.
- [20] J. Li, Y. Sun, J. Su, T. Suzuki, and F. Huang, in *International Conference on Artificial Intelligence and Statistics* (PMLR, 2020), pp. 504–515, 2001.05070.
- [21] K. Hartnett, *Foundations built for a general theory of neural networks* (2019), <https://www.quantamagazine.org/foundations-built-for-a-general-theory-of-neural-networks-> Accessed 8 July 2022.
- [22] J. E. T. Taylor and G. W. Taylor, *Psychonomic Bulletin & Review* **28**, 454 (2020).
- [23] A. W. Senior, R. Evans, J. Jumper, J. Kirkpatrick, L. Sifre, T. Green, C. Qin, A. Židek, A. W. Nelson, A. Bridgland, et al., *Nature* **577**, 706 (2020).
- [24] T. F. Brady, T. Konkle, G. A. Alvarez, and A. Oliva, *Proceedings of the National Academy of Sciences* **105**, 14325 (2008).
- [25] D. Shin, *International Journal of Human-Computer Studies* **146**, 102551 (2021).
- [26] H. Choung, P. David, and A. Ross, *International Journal of Human-Computer Interaction* pp. 1–13 (2022).
- [27] A. Hasija and T. L. Esper, *Journal of Business Logistics* (2022).
- [28] A. Marcianò, D. Chen, F. Fabrocini, C. Fields, E. Greco, N. Gresnigt, K. Jinklub, M. Lulli, K. Terzidis, and E. Zappala, *Neural Networks* **153**, 164 (2022).
- [29] E. Farhi and H. Neven, arXiv:1802.06002 (2018), URL <https://arxiv.org/abs/1802.06002>.
- [30] K. Beer, D. Bondarenko, T. Farrelly, T. J. Osborne, R. Salzmann, D. Scheiermann, and R. Wolf, *Nature communications* **11**, 1 (2020).
- [31] C. Fields, J. F. Glazebrook, and A. Marcianò, *Fortschritte der Physik* **70**, in press (2022).
- [32] P. L. Bartlett, A. Montanari, and A. Rakhlin, *Acta numerica* **30**, 87 (2021).
- [33] J. Frankle and M. Carbin, in *Proc. ICLR* (2019).
- [34] V. N. Vapnik and A. Y. Chervonenkis, *Theory of Probability & Its Applications* **26**, 532 (1982).
- [35] A. Blumer, A. Ehrenfeucht, D. Haussler, and M. K. Warmuth, *Journal of the ACM (JACM)* **36**, 929 (1989).
- [36] D. Haussler, in *The Mathematics of Generalization* (CRC Press, 2018), pp. 37–116.
- [37] M. Belkin, S. Ma, and S. Mandal, in *Proc. ICML* (PMLR, 2018), pp. 541–549.
- [38] T. Poggio, K. Kawaguchi, Q. Liao, B. Miranda, L. Rosasco, X. Boix, J. Hidary, and H. Mhaskar, arXiv:1801.00173 (2017), URL <https://arxiv.org/abs/1801.00173>.
- [39] C. Zhang, S. Bengio, M. Hardt, B. Recht, and O. Vinyals, in *Proc. ICLR* (Toulon, CS, France, 2017).
- [40] B. Neyshabur, R. Tomioka, and N. Srebro, in *Proc. ICLR Workshop* (2015).
- [41] K. Kawaguchi, L. P. Kaelbling, and Y. Bengio, arXiv 1710.05468 (2017), URL <https://arxiv.org/abs/1710.05468>.
- [42] S. Arora, R. Ge, Y. Liang, T. Ma, and Y. Zhang, in *Proc. ICML* (PMLR, 2017), pp. 224–232.



- [43] M. Belkin, D. Hsu, S. Ma, and S. Mandal, Proceedings of the National Academy of Sciences **116**, 15849 (2019).
- [44] B. Neyshabur, R. Tomioka, and N. Srebro, in *Conference on Learning Theory* (PMLR, 2015), pp. 1376–1401.
- [45] P. L. Bartlett, D. J. Foster, and M. J. Telgarsky, in *Proc. NIPS* (2017), vol. 30.
- [46] J. Shawe-Taylor, P. L. Bartlett, R. C. Williamson, and M. Anthony, IEEE transactions on Information Theory **44**, 1926 (1998).
- [47] P. L. Bartlett and S. Mendelson, Journal of Machine Learning Research **3**, 463 (2002).
- [48] C. Zhang, S. Bengio, M. Hardt, B. Recht, and O. Vinyals, Communications of the ACM **64**, 107 (2021), 1611.03530.
- [49] C. Rovelli, in *Journal of Physics: Conference Series* (IOP Publishing, 2011), vol. 314, p. 012006.
- [50] E. Bianchi, E. Magliaro, and C. Perini, Physical Review D **82**, 024012 (2010).
- [51] L. Kauffman, S. Lins, and S. Lins, *Temperley-Lieb Recoupling Theory and Invariants of 3-manifolds*, Annals of Mathematics Studies (Princeton University Press, 1994), ISBN 9780691036403.
- [52] C. Crnkovic and E. Witten, Class. Quant. Grav **5**, 1557 (1988).
- [53] C. Crnković, Nuclear Physics B **288**, 419 (1987).
- [54] C. Crnkovic, Classical and Quantum Gravity **5**, 1557 (1988).
- [55] J. Sawon, Geom. Topol. Monogr **8**, 145 (2006).
- [56] C. Rovelli and L. Smolin, Physical Review D **52**, 5743 (1995).
- [57] J. C. Baez, Advances in Mathematics **117**, 253 (1996).
- [58] K. Noui and A. Perez, Classical and Quantum Gravity **22**, 1739 (2005).
- [59] K. J. Friston, Nature Reviews Neuroscience **11**, 127 (2010).
- [60] K. J. Friston, Journal of The 1299 quantum mechanics, and then extending the analysis to Royal Society Interface **11**, 20130475 (2010).
- [61] K. J. Friston, arXiv:1906.10184 (2019), URL <https://arxiv.org/abs/1906.10184>.
- [62] C. Fields, K. J. Friston, J. F. Glazebrook, and M. Levin, Progress in Biophysics and Molecular Biology **173**, 36 (2022).
- [63] S. Shalev-Shwartz and S. Ben-David, *Understanding machine learning: From theory to algorithms* (Cambridge university press, 2014).
- [64] Y. Jiang, P. Natekar, M. Sharma, S. K. Aithal, D. Kashyap, N. Subramanyam, C. Lassance, D. M. Roy, G. K. Dziugaite, S. Gunasekar, et al., in *Proc. NeurIPS* (PMLR, 2021), pp. 170–190.
- [65] The capacity of a model, defined in Sec. V, specifies the hypothesis class from which a learning algorithm  $\mathcal{L}$  can choose a specific function  $h$ .